Hindawi
Advances in Meteorology
Volume 2022, Article ID 9102145, 15 pages
https://doi.org/10.1155/2022/9102145

Research Article

The Characteristics of Thunderstorms and Their Lightning Activity on the Qinghai-Tibetan Plateau

Lei Hui,[1] Yunjun Zhou ,[1,2] and Zhitao Yan[1]

[1]*Plateau Atmosphere and Environment Key Laboratory of Sichuan Province, College of Atmospheric Science, Chengdu University of Information & Technology, Chengdu 610225, China*
[2]*Collaborative Innovation Center on Forecast and Evaluation of Meteorological Disasters(CIC-FEMD), Nanjing University of Information Science & Technology, Nanjing, China*

Correspondence should be addressed to Yunjun Zhou; zhouyj@cuit.edu.cn

Received 4 July 2022; Revised 18 September 2022; Accepted 27 September 2022; Published 28 October 2022

Academic Editor: Marzuki Marzuki

Copyright © 2022 Lei Hui et al. This is an open access article distributed under the Creative Commons Attribution License, which permits unrestricted use, distribution, and reproduction in any medium, provided the original work is properly cited.

This paper discusses the temporal and spatial distribution characteristics of cloud-to-ground (CG) lightning activity over the Qinghai-Tibetan Plateau (QTP) from 2009 to 2018 and their dependence on meteorological factors. It is found that (1) the number of CG flashes fluctuates, reaches a maximum in 2014, and then gradually decreases. The main active period of CG lightning is from June to September each year, after which it decreases rapidly. CG lightning is mainly distributed in the valley areas at around 4800 m above sea level at Lhasa, Nagqu, and Chamdo, and there are differences in the characteristics of CG activity in these three areas. The peak of daily CG lightning occurs at 1000 UTC, and the lowest value is at 0400 UTC. The distribution of CG lightning in all seasons has obvious differences in peak time and the proportion of positive CG (+CG) lightning, with the ratio of +CG lightning to total CG lightning flashes in spring and autumn exceeding 50%. (2) The ratio of +CG lightning to total CG lightning flashes over the QTP is influenced by a combination of thermodynamic and microphysical factors. Over the QTP, greater vertical wind shear leads to the movement of upper positive charges and promotes the occurrence of +CG lightning. Also, the higher total column liquid water content implies higher cloud water content in the warm-cloud region, and the higher cloud-base height implies a thicker warm-cloud region, which is not conducive to the occurrence of +CG lightning. (3) During high-value years (in this study, 2010, 2012, 2014, and 2016), the midlatitude (30°N–60°N) high pressure is strong and the plateau is situated at the intersection of the East Asian and South Asian monsoons and the cold air from the northwest, which strengthens the water vapor convergence and increases the frequency of thunderstorms. When the plateau is under the control of the southerly monsoon from June to September every year, its atmosphere is full of water vapor and lightning activity is accordingly high, with the proportion of +CG lightning being about 10%. Meanwhile, in the remaining months, when controlled by the westerly wind belt, the plateau's water vapor condition is poor, the level of lightning activity weakens, and the proportion of +CG lightning gradually increases to more than 50%.

1. Introduction

Thunderstorms are a severe type of disastrous weather, usually accompanied by lightning, heavy rain, hail, and strong winds, and often impose serious impacts on people's everyday lives. Lightning is deadly and destructive to human productive life, and it also has a significant impact on a long time scale [1]. As an important phenomenon of thunderstorms, the distribution characteristics and patterns of lightning are indicative of the form and characteristics of thunderstorms.

Lightning has a significant impact on human society and kills hundreds of people worldwide each year. According to statistics, the number of deaths per million people in the United States has steadily declined to 0.1 since the 20th century, while in developing countries such as India, Zimbabwe, and Malawi, the number of deaths per million people remains greater than ten [2]. In addition to direct hazards, lightning also affects human society through indirect means. Lightning is one of the main factors in the destruction of trees and forests. A study by Abatzoglou et al.

showed that from 1992 to 2013, 40% of fires in the western United States were caused by lightning activity [3]. Veraverbeke et al. also showed that lightning was responsible for 75% of the fires over 200 ha in the boreal forests of the United States from 1975 to 2015 [4]. In addition, the damage and safety threats to aircraft from thunderstorms should not be underestimated.

The Qinghai–Tibetan Plateau (QTP), often referred to as the "Roof Of The World," is the highest plateau in the world, and its unique topography and geography have a critical impact on the global climate, especially in China. Meanwhile, the QTP is also one of the most active regions in the world in terms of lightning activity, with its average altitude reaching over 4000 m. The unique climatic and topographical conditions of the plateau make it a place with extremely high convective activity. In particular, thunderstorms are highly frequent in summer, and the frequency of strong thunderstorms is 3–5 times higher than that of Chengdu, Wuhan, and Shanghai at the same latitude [5]. Past studies have shown that the number of lightning flashes can be nine times greater south of the Himalayan foothills compared to the northern foothills and that topographic and latitudinal factors have an important influence on the distribution of lightning density, with cloud-to-ground (CG) lightning in western China mainly distributed in the basin belt [6]. Jicuomu et al. [7] showed that the strongest lightning activities along the QTP railroad occurred in 2013 and were mainly distributed over the areas of Lhasa and Shannan. Studies of lightning activity over the plateau have shown that the intensity of lightning discharges is weaker over the plateau than in other areas [8]. Meng et al. [9] studied the correlation between CG lightning and radar echo characteristics in the Nagqu region and found that the peak value of radar reflectivity in the Nagqu region tends to be concentrated in the range of 34–41 dBZ, indicating that thunderstorms are generally weak over the QTP, but with a higher frequency of positive CG (+CG) lightning. Zhang et al. [10] found that the ratio of +CG lightning to negative CG (−CG) lightning in the eastern part of the QTP was about 1:8, while Zhao et al. [11] analyzed summer thunderstorm processes in the Nagqu region and found that the +CG ratio was about 33%. Zhang et al. [12] showed that plateau thunderstorms are generally weak in intensity and short in duration, mainly occurring between 05:00 and 19:00 UTC. Guo et al. [13] found by simulating the thunderstorm process on the QTP that plateau thunderstorms have special characteristics: they have short life spans, smaller updrafts and downdrafts, and significantly more solid precipitation than liquid precipitation. Taken together, the previously mentioned studies demonstrate that thunderstorms on the QTP have special characteristics, and their unique forms are related to the QTP's special topographic and meteorological conditions.

There are many factors that influence thunderstorms, and human activity is one of them. Urbanization and air pollution are among the important factors, and Westcott's study shows that as urban population and city size increase, convective thunderstorms develop more frequently, and lightning occurs more frequently in years when pollution is heavier in larger cities [14]. A study of lightning characteristics in Bangladesh shows that the land cover categories have an influence on the characteristics of lightning. Waterbodies and herbaceous wetlands experienced enhanced lightning activity when compared to other land cover categories. More extensive irrigation activities on the land may have an important impact on the distribution characteristics of lightning [15]. Studies of rainfall in peninsular India also suggest that agricultural intensification may reduce rainfall in some parts of India during the monsoon season [16]. Studies by scholars on the characteristics of lightning activity in Athens have also shown that different land cover categories can have different effects on lightning activity [17]. Thus, human activities can have an important impact on the distribution characteristics of lightning through the modification of land cover categories and the emission of pollutants into the air.

Environmental factors have a significant influence on the presence of lightning activity characteristics, with studies revealing that the high liquid water content in the mixed-phase region reflects a high rime accretion rate of graupel particles, which leads to positive charges carried by graupel particles, in turn resulting in the generation of an inverted charge structure and high ratios of +CG lightning [18–26]. Zhang et al. [27] studied the characteristics of thunderstorms under four different altitudinal conditions and found that tripole-type thunderstorms occur mainly in the central part of the QTP and that the 2-m temperature difference at the surface and the air humidity before the occurrence of a thunderstorm make an important contribution to the formation of the positive charge center at its base.

Due to the frequent occurrence, short life history, and rapid movement of plateau thunderstorms and convection, existing studies on them have been limited by a lack of ground-level observational data and have instead had to rely solely on satellite observations to analyze their activities and characteristics, with most attention paid to cases in the areas of Qinghai and western Sichuan. Furthermore, studies have thus far mainly focused on the influence of the special charge structure of plateau thunderstorms, with research on the correlation between meteorological factors and plateau thunderstorm characteristics being insufficient. Lastly, to date, studies have lacked long-term data, meaning research findings on the characteristics of plateau thunderstorms have been limited to the analysis of relatively short time series.

To address these knowledge gaps, the present paper analyzes the spatial and temporal distribution characteristics of CG lightning over the QTP based on lightning data from 2009 to 2018 obtained from the rapidly developing and now mature National Lightning Monitoring and Positioning System. More specifically, we analyze the spatial and temporal distribution characteristics of CG lightning over the QTP in combination with reanalyzed data from the ERA5 dataset to study the characteristics of thunderstorms and lightning activities over the QTP region and the mechanisms underlying their generation. Not only does this study have a certain academic significance, but it also provides a theoretical basis for lightning protection over the QTP region.

2. Materials and Methods

2.1. CG Lightning Data. The CG lightning location data are from the ADTD (ground-based Advanced Time of Arrival and Direction CG lightning sensors) observation system of the QTP for the period 2009–2018. The ADTD lightning positioning system over the QTP consists of 24 observation sites with a single station detection range of 150 km, a detection efficiency of 94%, and a positioning accuracy of 500 m. The distribution of sites and the elevation of the QTP are shown in Figure 1. The data obtained from each station include the time of lightning occurrence, the polarity of the lightning, latitude and longitude, and the intensity of the lightning current. The data were quality-controlled according to methods in a previous study, in which anomalous data with intensity greater than 400 kA and +CG lightning with intensity less than 15 kA were excluded [28]. There are relatively fewer stations in the western part of the QTP, and the topography there is more complex than in the central and eastern parts, meaning the detection efficiency of lightning in the west is lower than that in the central and eastern QTP. Due to the lack of detection stations in the west, the shaded areas are not analyzed in this paper.

2.2. Environmental Factor Data. Previous studies have shown that various environmental factors, such as convective available potential energy (CAPE), vertical wind shear, cloud-base height (CBH), and zero-layer height, have significant effects on the presence of +CG lightning [29,30]. To discuss the association between the positive ground flash ratio and environmental factors over the QTP, 10 environmental factors between May and October, when lightning is frequent, were selected to discuss the correlation between +CG lightning flashes and environmental factors. These factors were classified into five thermodynamic and five moisture factors according to the principles of their influence. Previous studies have tended to focus on the eastern QTP, and there is a lack of research on the situation in the central and western QTP. The environmental factor data used in this paper are from the monthly averages of single-layer and baroclinic data from the ERA5 reanalysis dataset, with a spatial resolution of $0.25^{\circ} \times 0.25^{\circ}$. Due to the large topographic fluctuations over the QTP, the barometric data of ERA5 are not suitable for analyzing the vertical distribution of environmental factors, so this paper uses the barometric equation with elevation (digital elevation map) data to process the barometric layers as geometric heights above the ground and selects the barometric layer closest to 3 and 5 km to represent the environmental data at heights of 3 and 5 km above the ground surface. In this paper, the thermodynamic factors selected include CAPE, surface pressure, potential temperature (THETA), vertical wind shear from 0 to 3 km (SHEAR-3), and vertical wind shear from 0 to 5 km (SHEAR-5). Moisture factors include the dewpoint temperature difference (DPD), average relative humidity (RH) within 3–5 km, CBH, zero-degree layer height (ZDH), total column liquid water content (TCLW), and total column ice water content. THETA is calculated as

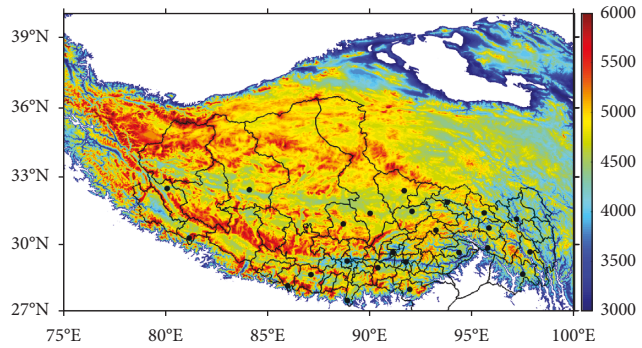

Figure 1: Distribution of lightning observation sites on the QTP (black dots) and the elevation of the region (color shading).

$$THETA = T_{2m}\left(\frac{P_0}{P}\right)^{0.286}, \tag{1}$$

where T_{2m} is the 2-m temperature, P0 is 1000 hPa, and P is the surface air pressure. SHEAR-3 and SHEAR-5 are calculated as

$$SHEAR = \sqrt{(u_1 - u_0)^2 + (v_1 - v_0)^2}, \tag{2}$$

where u_0, u_1, v_0, and v_1 are the longitudinal and latitudinal wind speeds at the two heights, respectively. DPD is the difference between the 2-m temperature and the 2-m dewpoint temperature, which is calculated as

$$DPD = T - T_d. \tag{3}$$

3. Results and Discussion

3.1. Characteristics of Lightning Activity at Different Time Scales

3.1.1. Annual Distribution of CG. The QTP is one of the most active regions in the world in terms of lightning activity, driven by its unique climatic and topographical conditions. Figure 2 shows the annual statistics of CG lightning on the QTP for the period 2009–2018. Figure 2(a) presents the annual distribution, in which the dashed line indicates the proportion of +CG lightning to total CG lightning, with total CG lightning showing a low–high–low staggered distribution from 2009 to 2016 and a slow decrease after 2016. The highest value of CG lightning occurred in 2014. As shown in Figure 2(a), the +CG lightning ratio over the QTP exceeds 10% in this decade, with the highest value (27%) in 2010. Figures 2(b) and 2(c) show the peak current distribution of +CG and −CG lightning during this decade, respectively. For + CG lightning, there are two peaks of lightning intensity, with a secondary peak interval at around 30 kA and a primary peak interval at around 80 kA. Compared with the peak current distribution of −CG lightning, the intensity distribution of +CG lightning is more uniform, with a large number of flashes distributed between 30 kA and 100 kA. The intensity distribution of −CG lightning is more concentrated, mainly around 30 kA, which is the only peak. After the intensity reaches its peak, the number of CG lightning flashes decreases rapidly.

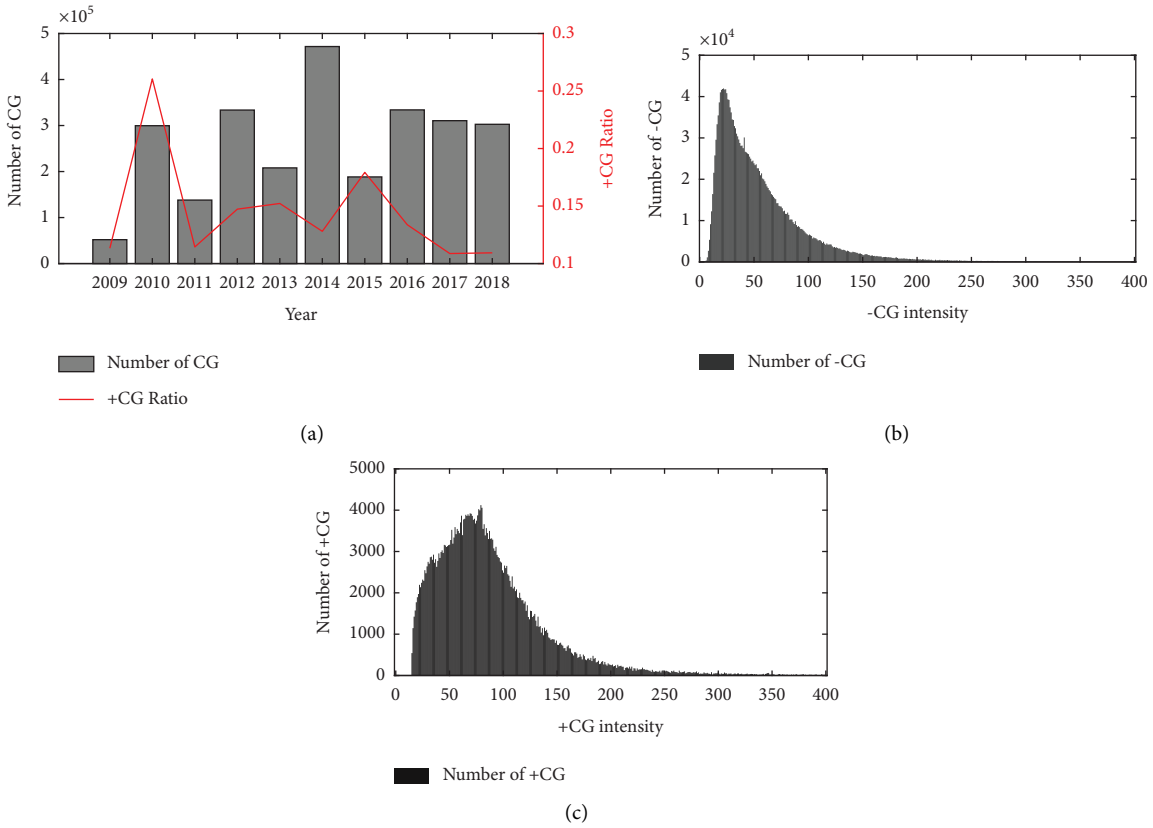

FIGURE 2: (a) Total number of CG lightning flashes from 2009 to 2018. The curve indicates the proportion of +CG lightning. (b, c) Intensity probability distributions of −CG and +CG lightning, respectively.

Figure 3(a) shows that CG lightning is distributed throughout the plateau but with a relatively sparser distribution in the west. In the central-eastern QTP, there are three distribution centers, at Lhasa, Nagqu, and Chamdo. Figure 3(b) shows that in the year with the least CG lightning (2009), the number of CG lightning flashes near Nagqu and Lhasa decreases significantly, with the maximum decrease being 200 flashes/year, and as shown in Figure 3(c), in the year with the most CG lightning (2014), CG lightning basically has an increasing trend, with the largest increase (500 flashes/year) in Lhasa and Chamdo. In the year with the highest CG lightning, the overall CG lightning on the plateau increases, with the largest increase in the regions of Lhasa and Chamdo at up to 500 times/year, while the number of CG lightning flashes in the Nagqu region decreases slightly compared with the average. In summary, although CG lightning is distributed across the plateau region as a whole, the CG lightning at Lhasa, Nagqu, and Chamdo varies the most dramatically, and its trend has an important influence on the overall trend of CG lightning over the QTP.

3.1.2. Monthly Distribution of CG Lightning. The distribution of QTP thunderstorms is not consistent throughout the year, being mainly concentrated in the rainy season. On the basis of the monthly CG lightning data statistics observed by ADTD from 2009 to 2018 (Figure 4), from June to September, the monthly distribution of CG lightning on the QTP is uneven, and the number of CG lightning flashes occurring in the four months accounts for more than 85% of the annual number. In these four months, it is mainly −CG lightning that occurs, and the average incidence of +CG lightning is less than 10%. However, the distribution of +CG lightning does not change much throughout the year compared to −CG lightning, and its trend is not the same as that of −CG lightning. In April, the most frequent month for + CG lightning, and from June to September, when the distribution of −CG lightning is concentrated, there are fluctuations in the number of +CG lightning flashes, but the overall change is not large, and the trend of +CG lightning decreases after September. Therefore, from June to September, the proportion of +CG lightning is less than 10%, while in the remaining months, the amount of −CG lightning decreases rapidly and that of +CG lightning decreases less or even increases, meaning the proportion of +CG lightning increases rapidly.

Based on the above distribution pattern, the intensities of +CG lightning from June to September and the remaining months are counted separately. Figures 4(b) and 4(c) show the peak current distribution of +CG lightning and −CG lightning in June and September during this decade. In these four months, the intensity of -CG lightning is concentrated at 30 kA, and the distribution pattern is consistent with the distribution pattern of the whole year. In contrast, the intensity of +CG lightning is concentrated at around 30 kA, which corresponds to the first peak of the annual distribution.

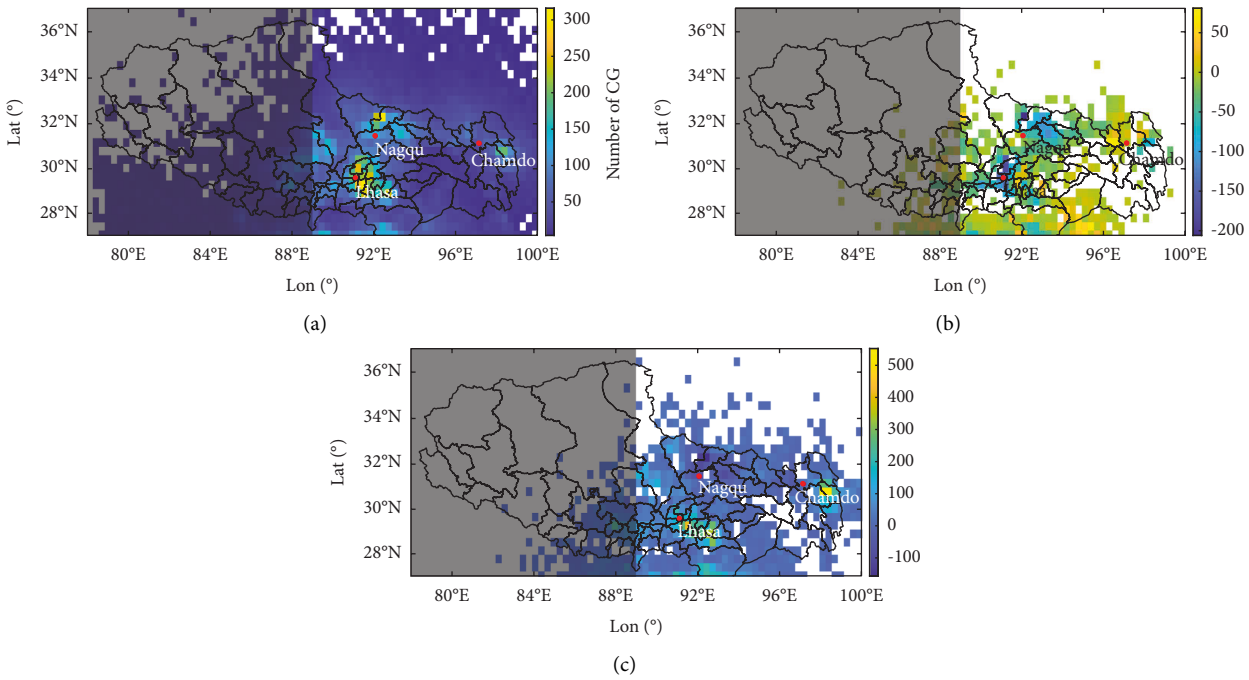

Figure 3: (a) Average distribution of CG lightning during 2009–2018. (b) Difference between the lowest year of CG lightning (2009) and the 10-year average. (c) Difference between the highest year of CG lightning (2014) and the 10-year average. The area of $0.1^{\circ} \times 0.1^{\circ}$ is taken as a unit area, and the area with less than 2 times/year is omitted from the statistics.

After that, the number of +CG lightning flashes gradually decreases with increasing intensity. The distribution range of +CG lightning is larger than that of −CG lightning, and there is a subpeak area near 80 kA. Figures 4(d) and 4(e) show the peak current distribution of +CG lightning and −CG lightning for the remaining months. The −CG lightning still has only one peak at 30 kA, and the distribution pattern is similar to the annual distribution. The + CG lightning peaks at 80 kA, so there are two peak areas of 30 kA and 80 kA in the annual distribution of CG lightning.

Considering that the CG lightning over the QTP is mainly concentrated in May–October, the CG lightning in these six months is selected for statistical discussion of the monthly distribution characteristics of CG lightning during this decade. Figures 5(a)–5(f) show the spatial distribution of CG lightning between May and October. In May, CG lightning is concentrated in the areas around Nagqu and Lhasa, and there is no CG lightning over the rest of the QTP, while from June to September, the amount of CG lightning increases significantly. From June to August, the locations of CG lightning begin to expand, and their maximum distribution is reached in August. Then, in September, the distribution of CG lightning starts to shrink, and the number of CG lightning flashes per unit area starts to decrease. By October, the number of CG lightning flashes decreases rapidly, and only a small amount of CG lightning occurs in the vicinity of Nagqu and Lhasa.

3.1.3. Daily Distribution of CG Lightning. Figure 6(a) presents the number of CG lightning flashes per hour throughout the day during 2009–2018. The peak total CG lightning occurs between 0900 and 1000 UTC, and there is a small peak at around 1900–2000 UTC. After that, the number of CG lightning flashes starts to decline, reaching its lowest value at 0300–0400 UTC, and then gradually increases. The trend of −CG lightning is basically the same as that of total flashes, while the +CG lightning peak occurs at around 1200 UTC, which is two hours later than the total CG lightning peak, and then the rest of the trend is basically the same as that of total CG lightning.

Figures 6(b)–6(e) illustrate the daily lightning-flash-number trends of the QTP in the four seasons. According to the climatic characteristics of the QTP, March to April is defined as spring, May to August as summer, September to October as autumn, and November to February as winter. During the spring, the CG lightning peak occurs daily from 1500 to 1700 UTC, with a secondary peak at 1300 UTC. The percentage of +CG lightning in spring is higher than 40%, with the highest value reaching 80% at around 1700 UTC. The distribution pattern of −CG lightning is the same as that of the whole year. In summer and autumn, the distribution of CG lightning is basically consistent with that throughout the year, and the daily subpeak at around 2000 UTC is more obvious in autumn than in summer. In winter, there are two peaks in the CG lightning distribution, at 1200 and 1900 UTC, and the number of +CG lightning flashes is greater than the number of −CG lightning flashes throughout the day. It can be seen that, across the four seasons, the change in total CG lightning is mainly caused by the change in −CG lightning, and that + CG lightning changes with the seasons, but the change is relatively small. In spring and winter, the percentage of +CG lightning is generally higher than 50%, and the highest values of +CG lightning occurrences are mainly distributed at around 1600–18 : 00 UTC.

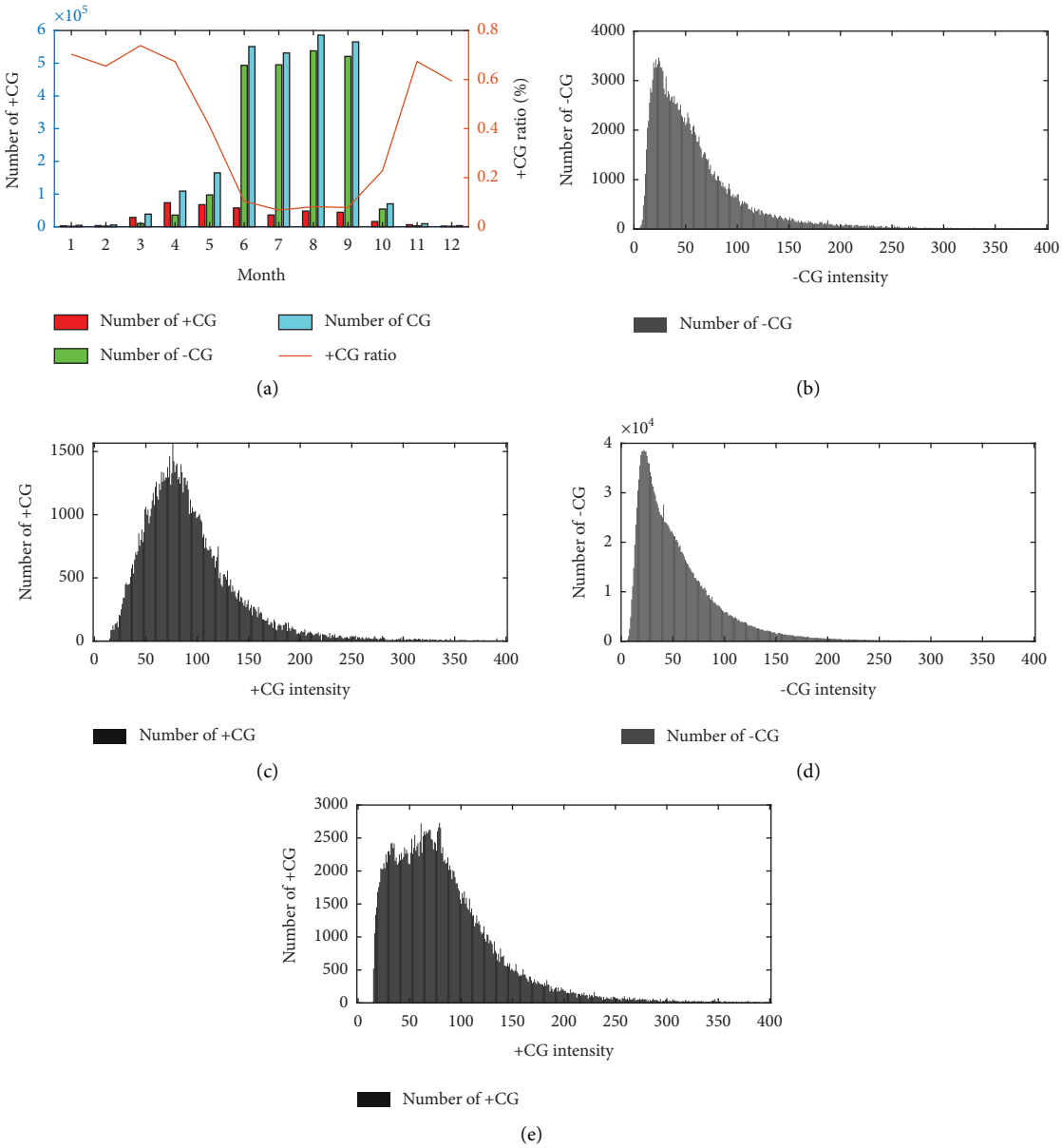

FIGURE 4: (a) Total number of +CG, −CG, and total CG lightning flashes in each month within 10 years, in which the broken line represents the proportion of +CG lightning in each month. (b, c) Probability distribution of −CG and +CG lightning intensity from June to September, respectively. (d, e) Probability distribution of −CG and +CG lightning intensity in other months.

3.2. Spatial Distribution Characteristics of Lightning Activity. Based on the statistics of the number of CG lightning flashes on the QTP during the study period, the occurrence of CG lightning on the QTP is mainly concentrated in the areas of Lhasa (29.2°N–31.0°N, 89.0°E–92.6°E), Nagqu (29.6°N–36.3°N, 83.6°E–95.5°E), and Chamdo (28.4°N–32.5°N, 93.6°E–99.1°E), and so, the following discussion concentrates on these places. Figure 7(a) gives the year-by-year statistics of the number of CG lightning flashes in these three locations during the period 2009–2018. Among the three sites, the number of CG lightning flashes and the percentage of +CG lightning at Lhasa and Chamdo have the same trend. The percentage of +CG lightning in the areas of Lhasa and Nagqu is within 10%, while at Chamdo, it is significantly higher, at more than 10% and even close to 20% in 2012. The CG lightning trend in the Nagqu region is the same as that in the Lhasa region, indicating that the changes in the number of CG lightning flashes are significantly influenced by the changes in the large-scale circulation situation across the QTP.

Figure 7(b) shows the month-by-month statistics of CG lightning in the three regions. The results show that CG lightning at all three locations is concentrated from June to September, and the number of CG lightning flashes in the remaining months is low, with only a few dozen occurrences in December and January. The proportion of +CG lightning is generally higher at Chamdo than at Nagqu and Lhasa. Outside of June to September, in terms of the overall trend of

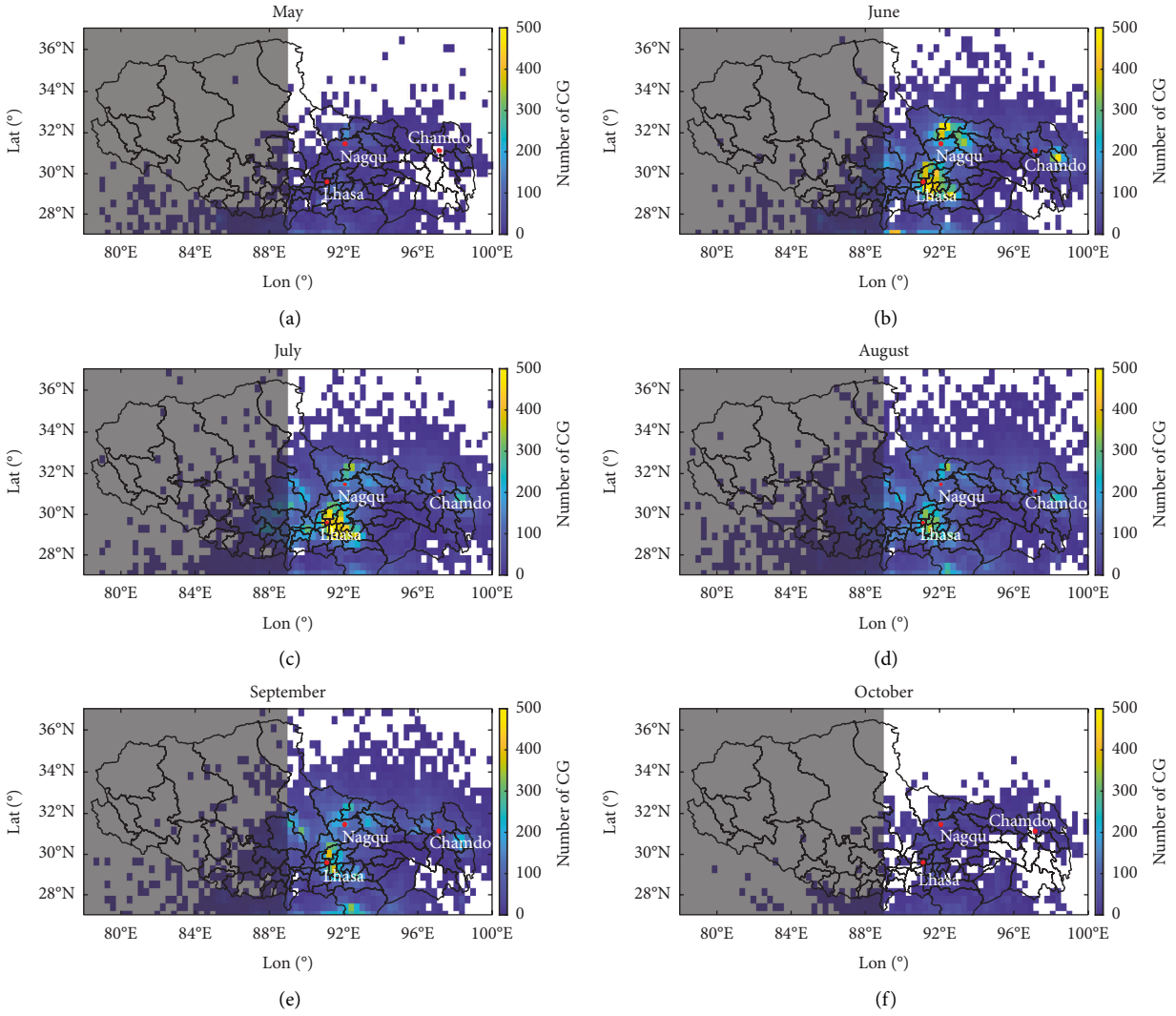

Figure 5: (a–f) Average distribution of CG lightning from May to October, respectively, during 2009–2018.

the months before and after the rise, more than 50% of the +CG lightning ratio is in January and December. The proportion of +CG lightning at Lhasa and Nagqu is generally around 10%, and the variation between months is not large, reaching its highest value of around 20% in April and November. Figure 7(c) compares the 24-hour CG lightning trends for the three locations. The CG lightning trends at Nagqu and Chamdo are consistent with the region-wide CG lightning trend, with most flashes occurring at 1000 UTC and the least at 0400 UTC. Meanwhile, in the area of Lhasa, while the lowest occurrence of ground flashes is also at 0400 UTC, its maximum appears at 1200 UTC, which is a delay of two hours compared with Nagqu and Chamdo. The proportion of +CG lightning is still significantly higher at Chamdo than at Lhasa and Nagqu, and the highest value, which can reach more than 40%, appears between 0300 and 0400 UTC. Then, the proportion gradually decreases to its lowest value at 0800 UTC before gradually increasing again. Note that even at its lowest level, the proportion of +CG lightning at Chamdo is about 20%, and at Lhasa and Nagqu, the 24-hour change is not an obvious one, being generally 10% or less.

Figure 8 shows the effect of altitude on the number of CG lightning flashes. It can be seen that CG lightning is sparsely distributed below 2500 m, and the first peak of the CG lightning distribution occurs at around 2500 m, which is due to the rapid uplift of the southern part of the QTP at roughly this height above sea level. The rapidly rising topography causes large quantities of water vapor and unstable energy to accumulate at the foot of the mountains, which results in frequent convective activity locally and the generation of a large amount of lightning activity. The number of CG lightning flashes then rises gradually with the elevation, reaching a peak near 4800–4900 m. Comparing the topography with the distribution map of CG lightning, it can be seen that CG lightning is mainly distributed in the valley areas between the Himalayas, Kunlun Mountains, and Hengduan Mountains. Solar radiation is strong in highland areas, and the terrain is complex and influenced by thermodynamic factors, so CG lightning occurs mostly in valley areas. The number of CG lightning flashes decreases after the altitude exceeds 5000 m.

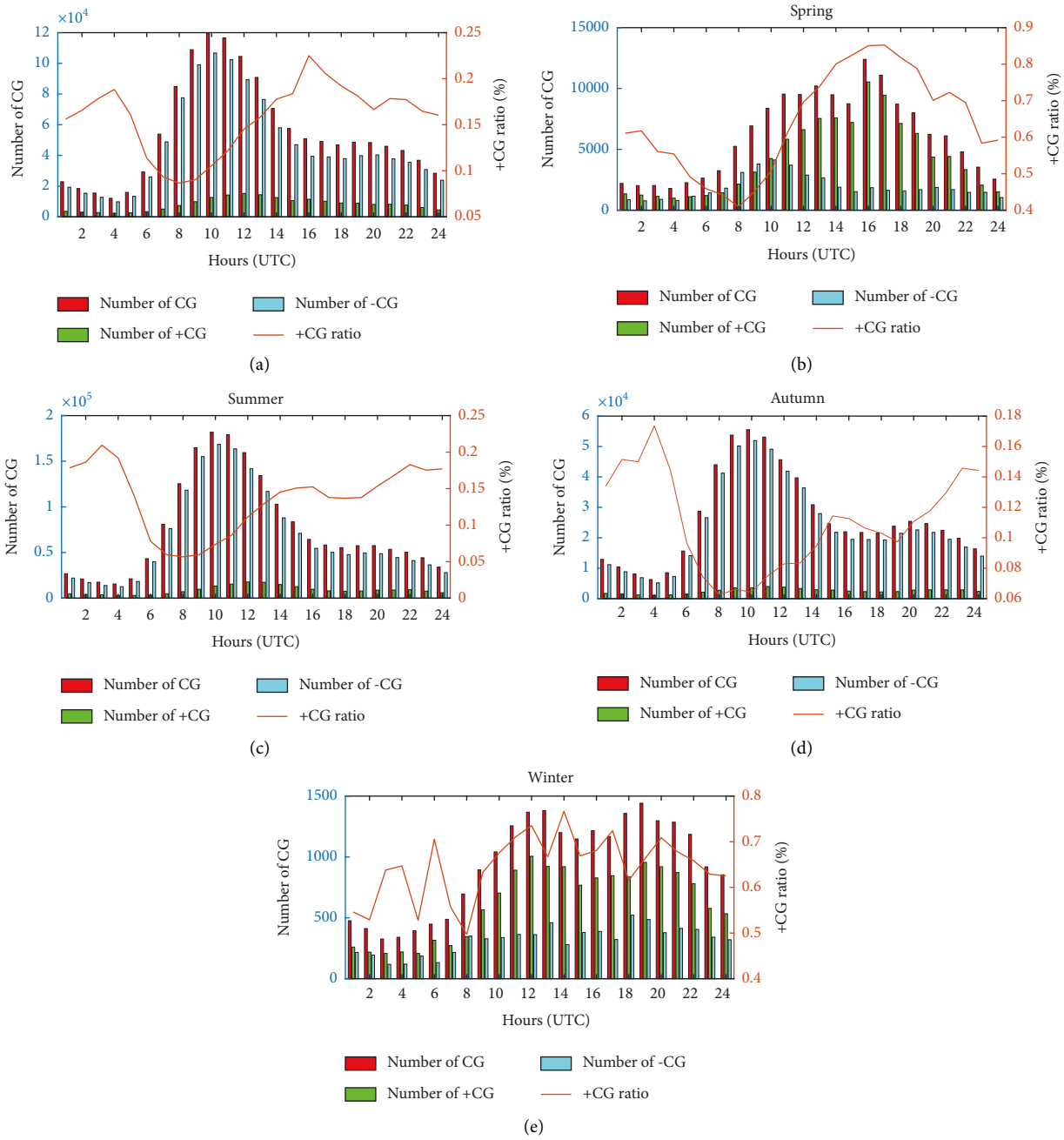

FIGURE 6: (a) Hourly distribution of the number of CG lightning flashes during 2009–2018. (b–e) Hourly distribution of the number of CG lightning flashes in the four seasons, in which the dashed line indicates the proportion of +CG.

3.3. Mechanistic Analysis of the Spatial and Temporal Distribution of Lightning Activity. As seen from the above results, the characteristics of lightning activity over the QTP are closely related to large-scale circulation and topographic factors. The former of these, i.e., the influence of large-scale circulation on lightning activity, is discussed next.

The annual series of the number of CG lightning flashes over the QTP was normalized to filter out the high-value years (2010, 2012, 2014, and 2016) and low-value years (2009, 2011, and 2013), and then the low-value and high-value years of 500-hPa geopotential height and wind field anomalies along with the number of CG lightning flashes in June–September were analyzed (Figure 9). The results show that the 500-hPa geopotential height anomaly in the high-value years is opposite in phase to that in the low-value years. During the high-value years, the high pressure along the line from midlatitude Central Asia to the southeast coastal area of China is strong, the cold air from Siberia is blocked near Qinghai and Gansu, the QTP is mainly controlled by the southerly wind direction, and the water vapor from the South China Sea and the Indian Ocean provides sufficient conditions for the occurrence of thunderstorms. The northwestern part of the QTP is mainly controlled by northwesterly winds, and the dry and cold airflow meets

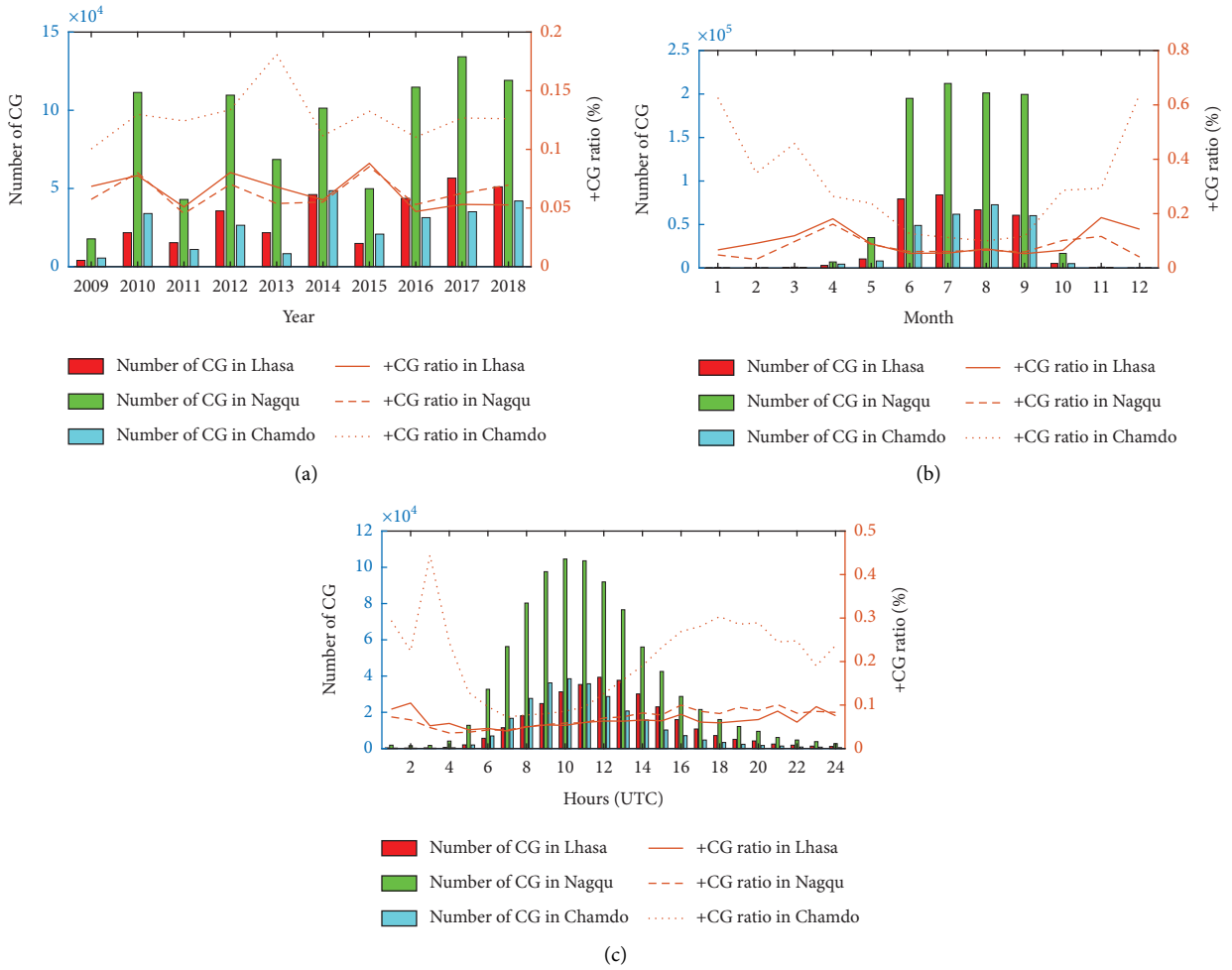

FIGURE 7: The (a) annual, (b) monthly, and (c) daily distributions of CG lightning in the areas of Lhasa, Nagqu, and Chamdo from 2009 to 2018.

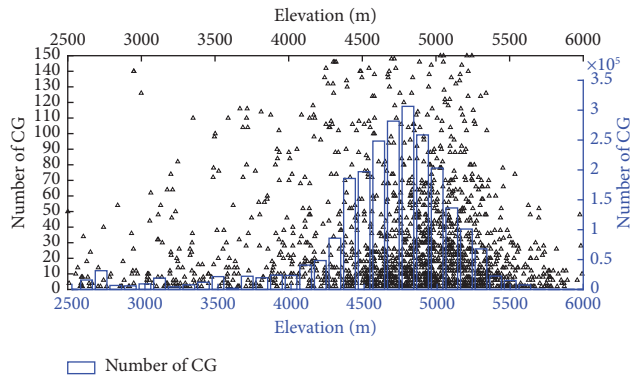

FIGURE 8: Number of CG lightning flashes per $0.25^\circ \times 0.25^\circ$ of elevation (triangles) and per 100 m (bars).

with the warm and humid airflow from the south in the central part of Tibet, which is favorable for the occurrence of strong convective weather such as thunderstorms. In contrast, in the low-value years, there are two ridges and one trough at high latitudes: one ridge each exists in the Ural Mountains and northern Japan, and the large trough in the middle guides the cold air southward from Siberia. The wind field shows that the QTP is mainly controlled by northerly winds in low-value years, while the East Asian monsoon and the South Asian monsoon stay in eastern China and India and have less influence on the plateau. The lack of water vapor transport and the lack of wind shear over the QTP are not conducive to the occurrence of thunderstorms.

Based on the above-mentioned data, it is known that lightning over the QTP mainly occurs between May and October. Therefore, the variation in the wind field between

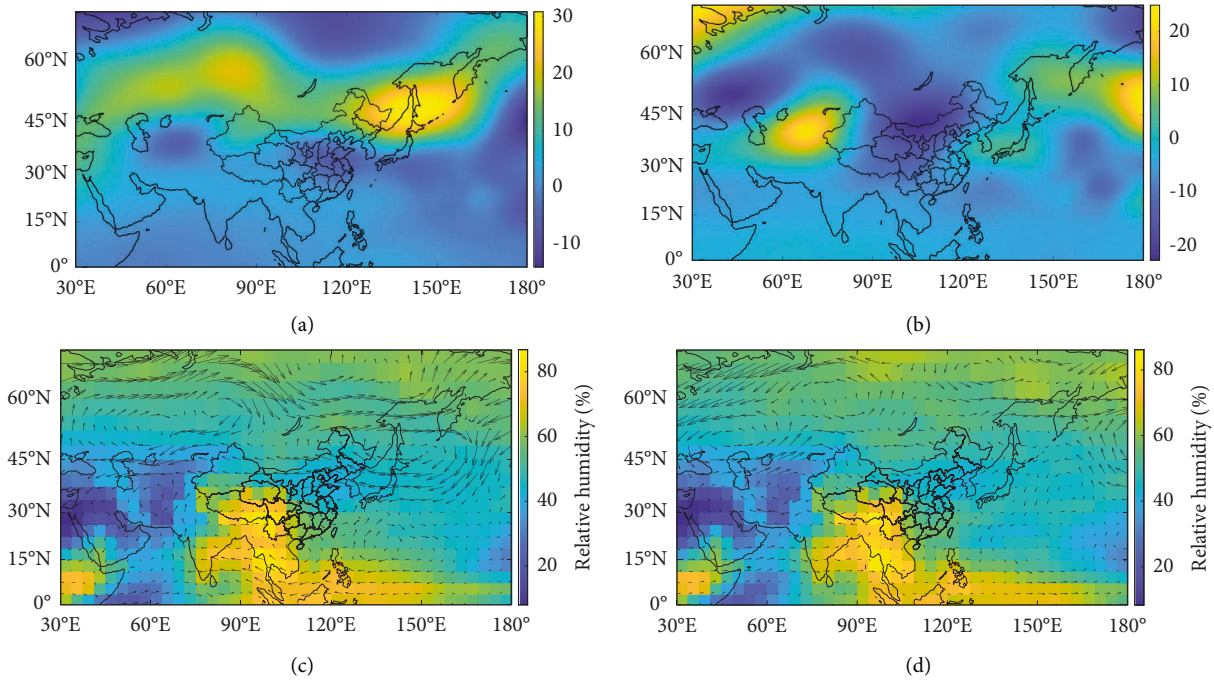

Figure 9: (a)~(b) The distance between the 500 hPa pressure field in the high and low ground-flash years; (c)~(d) 500 hPa wind field averages for high-value and low-value years, and the color-filled graphs are relative humidity averages.

those months, based on ECWMF reanalysis data, is presented in Figure 10, as well as color-filled graphs indicating the RH. In May, most of the 500-hPa wind field over the QTP is controlled by the westerly wind belt, with the exception being the Hengduan Mountains under the control of southwesterly winds, when the CG lightning activity is generally low. At this time, water vapor over the plateau is not abundant, except in the southwest region, and in the central and western regions of the QTP as a whole, the value is below 50%, which is not conducive to the occurrence of lightning. By June, the Indian monsoon strengthens, the eastern part of the QTP gradually turns to be controlled by the southwest wind, and the water vapor near the areas of Lhasa and Nagqu reaches 70%, at which point CG lightning starts to enter a period of frequent occurrence. Between July and August, the summer wind gradually strengthens, reaching its strongest point in August, and the central and western part of the QTP also turns out to be controlled by the southwest monsoon. The RH of the main part of the QTP reaches more than 80%. In September, the summer winds weaken, and the amount of water vapor transported from the Indian Ocean decreases. However, most parts of the QTP are still controlled by the southwest winds, and the RH in the western mountainous areas decreases to about 50%. Meanwhile, water vapor remains abundant in the central and western parts, and the RH at Lhasa and Nagqu continues to reach more than 70%, meaning the distribution of CG lightning in September contracts towards the central region relative to August, but the number of lightning occurrences is still high. In October, the main wind direction of the QTP shifts back to the control of the westerly wind belt, and the RH drops rapidly, with high-value areas only found to the south of the Hengduan Mountains, with lightning activity also weakening rapidly.

In summary, in high-value years of CG lightning occurrence, the midlatitude high pressure is strong, and the QTP is located at the intersection of the East Asian and South Asian monsoons and the cold air from the northwest, which strengthens water vapor convergence and increases the frequency of thunderstorms. In low-value years, the circulation situation is the opposite, with the QTP mainly controlled by the dry and cold air from the north, which results in fewer thunderstorms. When the QTP is controlled by the prevailing westerly winds, the overall ground flash activity is weak, whereas when the winds change to summer winds from June to September, the plateau is full of water vapor and lightning is more active. The change in the wind field significantly affects the spatial and temporal distribution characteristics of CG lightning.

3.4. Correlation between CG Lightning Polarity and Environmental Factors. The occurrence and development of lightning are influenced by various meteorological factors, and microphysical and thermodynamic conditions have important effects on thunderstorms. In order to discuss the above characteristics of the CG lightning distribution, the relationship between the lightning density over the QTP and each factor is analyzed separately in this paper. The statistical range is the main concentration of CG lightning over the plateau (27,0°N–33.0°N, 84.0°E–100.0°E), and within this range, ERA5 reanalysis data and monthly averages of CG lightning occurrences over a 10-year period are used.

Generally speaking, +CG lightning occupies about 10% of all CG lightning. The statistics mentioned previously show that + CG lightning over the QTP accounts for a high percentage; plus, the intensity data are stronger than

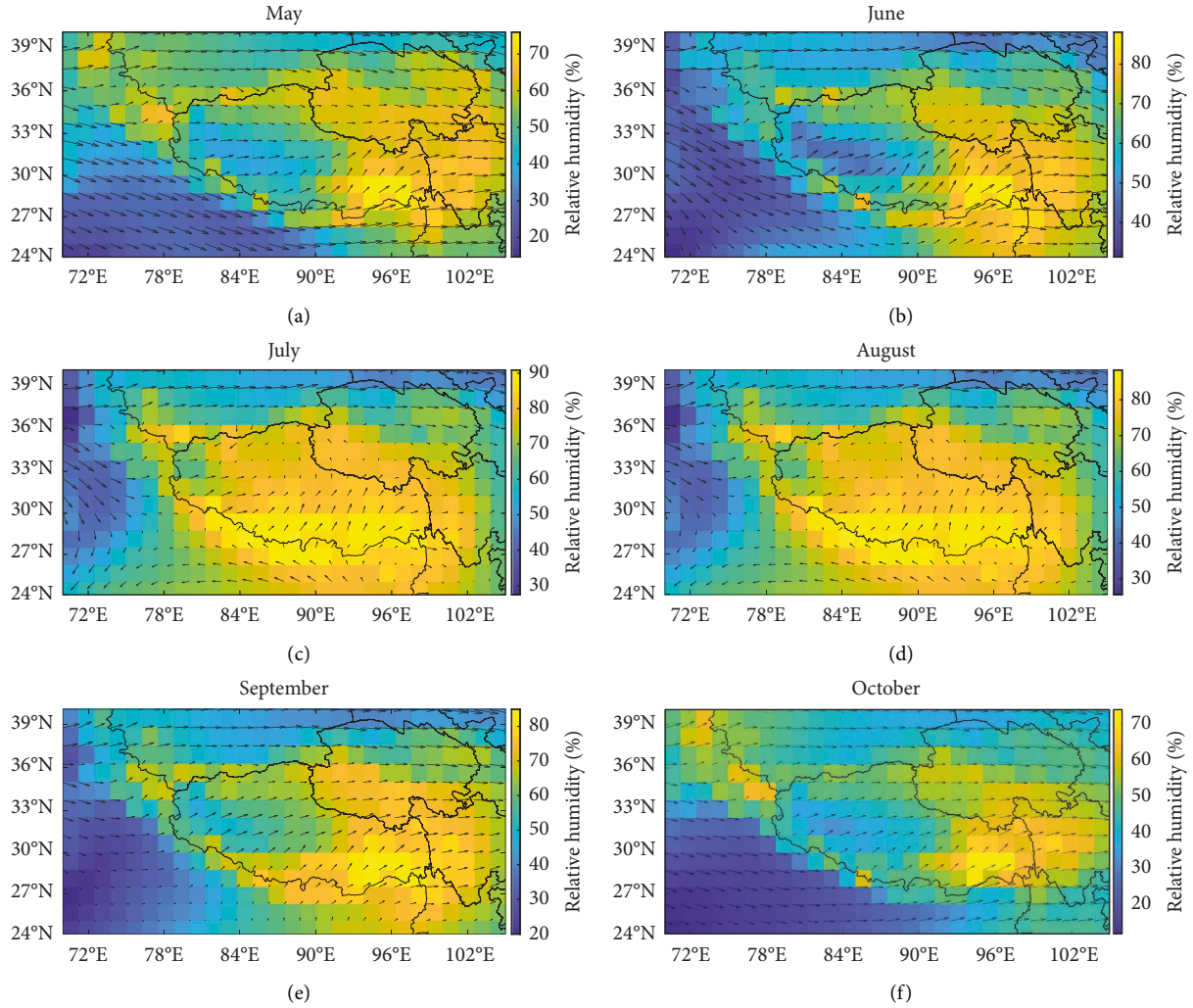

Figure 10: Average wind fields from (a) May to (f) October during 2009–2018. The color-filled plots are the average RH.

for −CG lightning, meaning more damage can be caused, so its distribution pattern is of great significance. Since CG lightning over the QTP mainly occurs between May and October, the proportion of +CG lightning flashes in these five months was selected for analysis with respect to environmental factors. Figure 11 shows the correlation between the frequency of +CG lightning and thermodynamic factors over the QTP between May and October. It can be seen that CAPE (Figure 11(a)), surface pressure (Figure 11(b)), and THETA (Figure 11(c)) show a significant negative correlation with the frequency of +CG lightning in the eastern part of the QTP. Previous studies suggest that strong thermodynamic conditions are favorable for the occurrence of +CG lightning and that strong updrafts will transport a large amount of water vapor to the mixed-phase region, which is favorable for particles to carry positive charges, and therefore, +CG lightning will increase [16–18]. In the present study, it is found that strong thermodynamic conditions are not favorable for the generation of +CG lightning, which may be due to the fact that weaker thunderstorms are more likely to generate positive charges over the QTP. The weaker the thermodynamic conditions, the higher the proportion of +CG lightning, and therefore, more +CG lightning tends to be produced during the dissipation phase of thunderstorms. The negative correlation between surface pressure intensity and the proportion of +CG lightning indicates that a certain thunderstorm intensity is required for the production of +CG lightning thunderstorms. The positive correlation between SHEAR-5 (Figure 11(d)) and SHEAR-3 (Figure 11(e)) shows a positive correlation with the proportion of +CG lightning, indicating that stronger vertical wind shear has a facilitating effect on the generation of +CG lightning. Strong vertical wind shear in thunderstorm clouds leads to tilting of the clouds, which favors tilting of the main positive charge region in the upper layer of the thunderstorm and avoids the lower negative charge region from blocking the discharge of positive charges, which is more conducive to the discharge of positive charges to the ground to generate +CG lightning. This is consistent with the previous work in which it was suggested that wind shear-induced displacement of ice-phase particles containing positive charges in the upper layer is an important cause of +CG lightning.

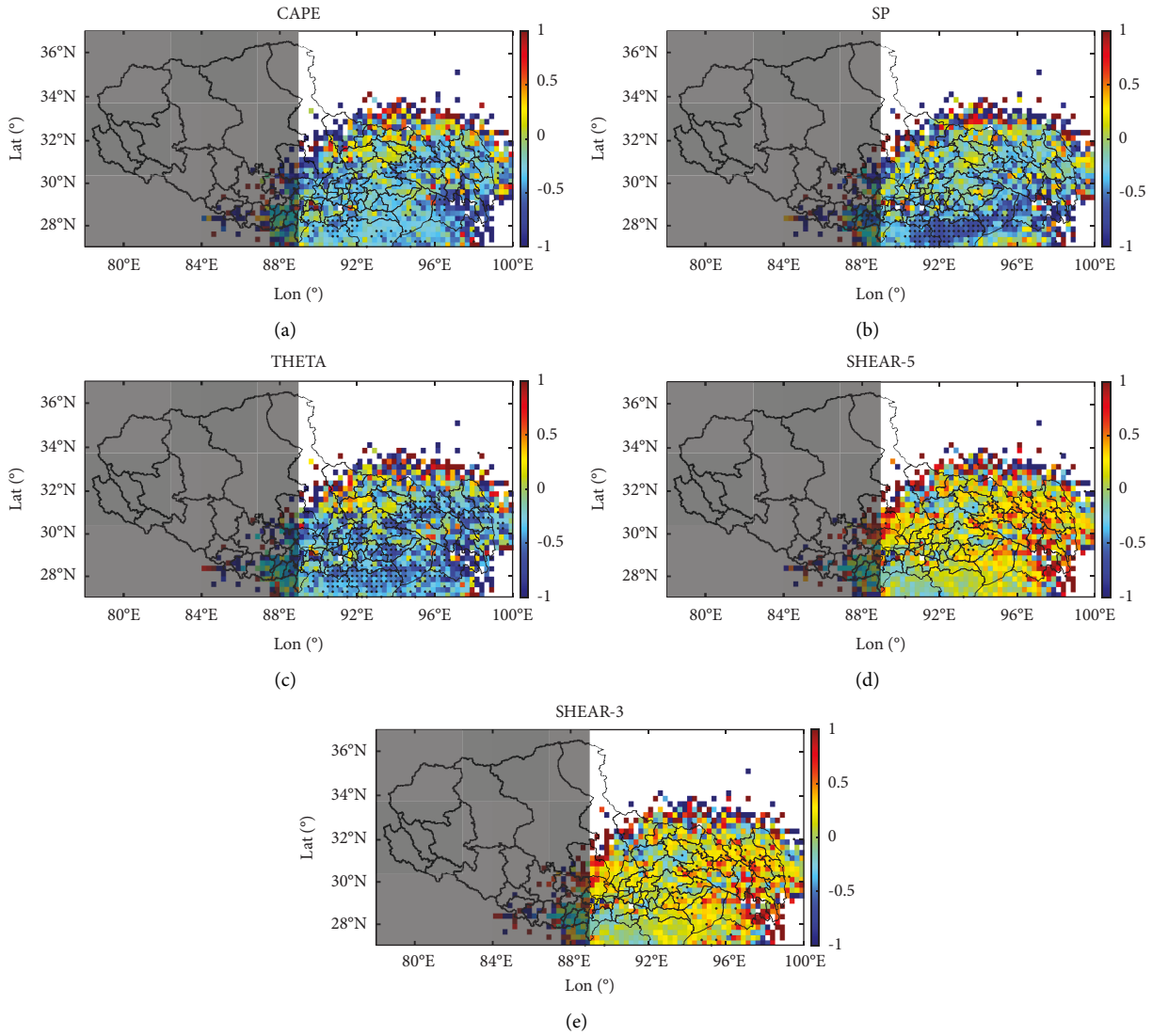

Figure 11: Correlation coefficients between the proportion of +CG (%) and (a) CAPE (J/kg), (b) SP (hPa), (c) THETA (K), (d) SHEAR-5 (m/s), and (e) SHEAR-3 (m/s) between May and October, the correlation coefficients in the figure are calculated based on the monthly average data of 60 months, and the black dots in the figure indicate that the point passed the 95% significance test.

Figure 12 shows the correlation between the water vapor condition factors and the proportion of +CG lightning over the QTP. DPD (Figure 12(a)), RH (Figure 12(b)), and CBH (Figure 12(c)) show a significant positive correlation with the proportion of +CG lightning. Among them, DPD and RH represent the temperature and humidity conditions in the lower troposphere. The positive relationship between CBH and +CG lightning indicates that a higher CBH is more favorable for the occurrence of +CG lightning. There is a clear linear relationship between CBH and updraft strength [31,32], with higher updrafts thought to be stronger, which facilitates the transport of water vapor to the mixed-phase region. A higher CBH also implies thinner warm clouds and that water vapor is more easily transported to the mixed-phase region above zero degrees. The high water vapor content in the mixed-phase region leads to positively charged shrapnel particles in the middle layer, which is more favorable for + CG lightning. ZDH (Figure 12(d)) and TCLW (Figure 12(e)) show a significant negative correlation with the proportion of +CG lightning. A higher ZDH indicates the presence of a thicker warm-cloud region, which is not conducive to the transport of water vapor to the mixed-phase region and therefore to the production of +CG lightning. For TCLW, the average cloud thickness and warm-cloud thickness are thinner in the highlands than in other regions owing to the higher average altitude. Also, the convective clouds are shallower than in other regions at the same latitude, and the warm-cloud thickness is thicker at the higher surface of the TCLW, which is not conducive to the transport of water vapor to the mixed-phase region and the generation of +CG lightning.

In summary, the thermodynamic and water vapor factors have an important influence on the proportion of +CG lightning, and both have positive and negative influences. Environmental factors have a significant influence on the spatial and temporal distribution characteristics of lightning.

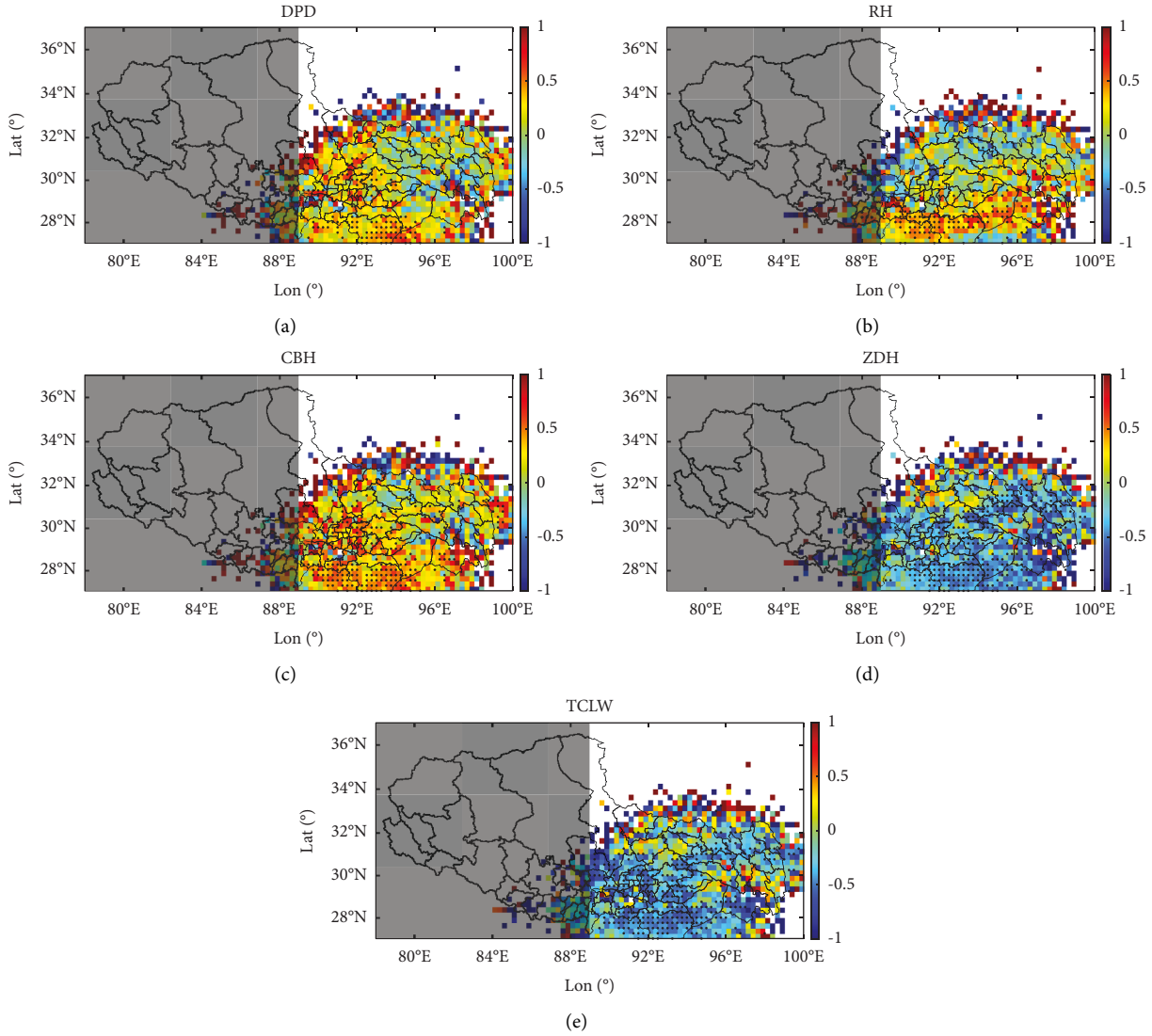

Figure 12: Correlation coefficients between the proportion of +CG (%) and (a) DPD (K), (b) RH (%), (c) CBH (m), (d) ZDH (m), and (e) TCLW (kg/m^2) between May and October. The correlation coefficients are calculated based on the monthly average data of 60 months, and the black dots indicate statistical significance at the 95% confidence level.

4. Conclusions

The following conclusions were obtained from an analysis of CG lightning observation data over the QTP for the period 2009–2018 along with ERA5 reanalysis data:

(1) CG lightning fluctuations over the QTP varied during 2009–2018, reaching the highest value in 2014. The percentage of +CG was 10%–25%. +CG and −CG have different peak intervals, respectively. There are obvious spatial and temporal characteristics of the ground flash distribution over the Qinghai-Tibet Plateau. The CG lightning distribution is mainly centered in the areas of Lhasa and Nagqu, and there is a subcenter at Chamdo. CG lightning is mainly distributed in valley areas at around 4800 m above sea level. CG lightning is mainly concentrated in the months of June to September, during which the proportion of +CG lightning is less than in other months. There are obvious differences in the distribution characteristics of CG lightning among the four seasons.

(2) There are obvious differences in the spatial and temporal distribution characteristics of CG lightning in Lhasa, Nagqu, and Chamdo, where CG lightning is concentrated. This may be related to the unique local topographic features.

(3) The proportion of +CG lightning over the QTP region is influenced by a combination of thermodynamic and microphysical factors. Both thermodynamic and microphysical factors have both positive and negative influences on the proportion of +CG lightning.

(4) The spatial and temporal distribution characteristics of CG lightning over the QTP are significantly influenced by the large-scale circulation system.

Data Availability

The data used to support the findings of this study are available from the corresponding author upon request.

Conflicts of Interest

The authors declare that they have no conflicts of interest.

Acknowledgments

This research was jointly supported by the Second Qinghai-Tibet Plateau Comprehensive Scientific Research Project (2019QZKK0104), the National Natural Science Foundation of China Project (41875169), the Sichuan Science and Technology Program Project (2022YFS0545), Guizhou Science and Technology Program Project Qiankehe Support ((2019) No. 2387), and Guizhou Science and Technology Program Project Qiankehe Support ((2022) No. 206), the Yunnan Science and Technology Program Project (202203AC100021).

References

[1] Y. Yair, "Lightning hazards to human societies in a changing climate," *Environmental Research Letters*, vol. 13, no. 12, Article ID 123002, 2018.

[2] R. L. Holle, "A summary of recent national-scale lightning fatality studies," *Weather, Climate, and Society*, vol. 8, no. 1, pp. 35–42, 2016.

[3] J. T. Abatzoglou, C. A. Kolden, A. P. Williams, J. A. Lutz, and A. M. S. Smith, "Climatic influences on interannual variability in regional burn severity across western US forests," *International Journal of Wildland Fire*, vol. 26, no. 4, pp. 269–275, 2017.

[4] S. Veraverbeke, B. M. Rogers, M. L. Goulden et al., "Lightning as a major driver of recent large fire years in North American boreal forests," *Nature Climate Change*, vol. 7, no. 7, pp. 529–534, 2017.

[5] Y. Zhang, X. Qie, M. Yan et al., "Preliminary analysis on formation of electrical characteristics of thumderstorm in different altitude regions in Chinese inland plateau," *Plateau Meteorology*, vol. 28, no. 5, pp. 1006–1017, 2009, in Chinese.

[6] M. Ma, S. Tao, B. Zhu, and W. Lu, "Climatological distribution of lightning density observed by satellites in China and its circumjacent regions," *Science in China—Series D: Earth Sciences*, vol. 48, no. 2, pp. 219–229, 2005.

[7] D. Jicuomu, G. Zhou, N. Mashida, L. Zejun, W. Jun, and W. Jiawei, "Research on lightning activity at high altitude in Tibet," in *Proceedings of the 2019 11th Asia-Pacific International Conference on Lightning*, Hong Kong, China, 2019.

[8] X. Qie and R. Toumi, "Lightning activities on qinghai-xizang plateau as observed by satellite-based lightning imaging sensor," *Plateau Meteorology*, vol. 22, no. 3, pp. 288–294, 2003, in Chinese.

[9] Q. Meng, P. Fan, D. Zheng, Y. Zhang, and W. Yao, "Relationships between cloud-to-ground lightning and radar parameters at Naqu of the Qinghai-Tibet Plateau," *Journal Of Applied Meteorological Science*, vol. 29, no. 5, pp. 524–533, 2018, in Chinese.

[10] Y. Zhang, Z. Ge, C. Cheng, and Q. Meng, "Electrical characteristics of atmosphere in east area of qinghai-xizang plateau," *Plateau Meteorology*, vol. 17, no. 2, pp. 26–32, 1998, in Chinese.

[11] Y. Zhao, Z. Zhang, W. Dong, H. Zhang, C. Chen, and T. Zhang, "Preliminary analysis of characteristics of lightning in the Nagqu area of the Qingha-i Xizang plateau," *Chinese Journal of Geophysics*, vol. 47, no. 3, pp. 405–410, 2004.

[12] C. Zhang, M. Yan, W. Dong, and Y. Zhang, "Analyses on atmospheric stratificati on characteristics of thunderstorms over qinghai-xizang plateau," *Plateau Meteorology*, vol. 24, no. 5, pp. 741–747, 2005.

[13] F. Guo, Y. Li, M. Bao, Z. Liu, Z. Huang, and M. Wang, "Effects of convection strength on the charge structure in a thunderstorm cell," *Science Technology and Engineering*, vol. 17, no. 25, pp. 7–16, 2017.

[14] N. E. Westcott, "Summertime cloud-to-ground lightning activity around major midwestern urban areas," *Journal of Applied Meteorology*, vol. 34, no. 7, pp. 1633–1642, 1995.

[15] A. Dewan, K. M. Islam, T. R. Fariha et al., "Spatial pattern and land surface features associated with cloud-to-ground lightning in Bangladesh: an exploratory study," *Earth systems and environment*, vol. 6, pp. 1–15, 2022.

[16] D. Niyogi, C. Kishtawal, S. Tripathi, and R. S. Govindaraju, "Observational evidence that agricultural intensification and land use change may be reducing the Indian summer monsoon rainfall," *Water Resources Research*, vol. 46, no. 3, 2010.

[17] V. Kotroni and K. Lagouvardos, "Lightning occurrence in relation with elevation, terrain slope, and vegetation cover in the Mediterranean," *Journal of Geophysical Research*, vol. 113, no. D21, Article ID D21118, 2008.

[18] C. P. R. Saunders and S. L. Peck, "Laboratory studies of the influence of the rime accretion rate on charge transfer during crystal/graupel collisions," *Journal of Geophysical Research: Atmospheres*, vol. 103, no. D12, pp. 13949–13956, 1998.

[19] W. D. Rust and D. R. MacGorman, "Possibly inverted-polarity electrical structures in thunderstorms during STEPS," *Geophysical Research Letters*, vol. 29, no. 12, p. 1571, 2002.

[20] T. Takahashi and K. Miyawaki, "Reexamination of riming electrification in a wind tunnel," *Journal of the Atmospheric Sciences*, vol. 59, no. 5, pp. 1018–1025, 2002.

[21] T. J. Lang, L. J. Miller, M. Weisman et al., "The severe thunderstorm electrification and precipitation study," *Bulletin America Meteorology Social*, vol. 85, no. 8, pp. 1107–1126, 2004.

[22] K. C. Wiens, S. A. Rutledge, and S. A. Tessendorf, "The 29 June 2000 supercell observed during STEPS. Part II: lightning and charge structure," *Journal of the Atmospheric Sciences*, vol. 62, no. 12, pp. 4151–4177, 2005.

[23] C. Emersic and C. P. R. Saunders, "Further laboratory investigations into the Relative Diffusional Growth Rate theory of thunderstorm electrification," *Atmospheric Research*, vol. 98, no. 2-4, pp. 327–340, 2010.

[24] L. D. Carey and K. M. Buffalo, "Environmental control of cloud-to-ground lightning polarity in severe storms," *Monthly Weather Review*, vol. 135, no. 4, pp. 1327–1353, 2007.

[25] D. R. MacGorman, A. J. Eddy, C. R. Homeyer, and E. Williams, "Environmental conditions producing thunderstorms with anomalous vertical polarity of charge structure," in *Proceedings of the 25th International Lightning Detection Conference & 7th International Lightning Meteorology Conference*, Florida, USA, 2018.

[26] S. B. Smith, J. G. LaDue, and D. R. MacGorman, "The relationship between cloud-to-ground lightning polarity and surface equivalent potential temperature during three tornadic outbreaks," *Monthly Weather Review*, vol. 128, no. 9, pp. 3320–3328, 2000.

[27] Y. Zhang, X. Qie, and M. Yan, "The ligntning characteristics of thunderstorm over Tibetan plateau and its origin discussion," *Plateau Meteorology*, vol. 26, no. 4, pp. 774–782, 2007.

[28] P. Zhao, H. Xiao, C. Liu, and Y. Zhou, "Dependence of warm season cloud-to-ground lightning polarity on environmental conditions over sichuan, southwest China," *Advances in Meteorology*, vol. 2021, Article ID 1500470, 2021.

[29] P. Zhao, H. Xiao, C. Liu, Y. Zhou, X. Xu, and K. Hao, "Evaluating a simple proxy for climatic cloud-to-ground lightning in Sichuan Province with complex terrain, Southwest China," *International Journal of Climatology*, vol. 42, pp. 3909–3927, 2022.

[30] P. Zhao, H. Xiao, J. Liu, and Y. Zhou, "Precipitation efficiency of cloud and its influencing factors over the Tibetan plateau," *International Journal of Climatology*, vol. 42, pp. 416–434, 2022.

[31] M. Brook, M. Nakano, P. Krehbiel, and T. Takeuti, "The electrical structure of the Hokuriku winter thunderstorms," *Journal of Geophysical Research*, vol. 87, no. C2, pp. 1207–1215, 1982.

[32] Y. Zheng and D. Rosenfeld, "Linear relation between convective cloud base height and updrafts and application to satellite retrievals," *Geophysical Research Letters*, vol. 42, no. 15, pp. 6485–6491, 2015.